

# Supplementary Material for: Smooth and border-collision characteristics of the bifurcation to alternans in paced cardiac tissue

Carolyn M. Berger,<sup>\*§</sup> Xiaopeng Zhao,<sup>†§</sup> David G. Schaeffer,<sup>‡§</sup> Hana M. Dobrovolny,<sup>\*</sup>  
Wanda Krassowska,<sup>†§</sup> and Daniel J. Gauthier<sup>\*†§</sup>

<sup>\*</sup>Department of Physics, <sup>†</sup>Department of Biomedical Engineering, <sup>‡</sup>Department of Mathematics, and <sup>§</sup>Center for Nonlinear and Complex Systems, Duke University, North Carolina, 27708 USA

In this supplementary material, we present additional data to support the claims made in the associate Letter [1]. Specifically, we show the temporal evolution of the transmembrane potential for two different pacing rates where the  $\Gamma$  versus  $\delta$  trends are substantially different, and we present all of our data showing  $\Gamma$  as a function of perturbation size  $\delta$ .

## Transmembrane Potential

The action potential duration (APD) quantifies the dynamical state of the tissue. To measure APD for these experiments, a glass microelectrode pulled to a resistance of  $\sim 20 \text{ M}\Omega$  is inserted into the cell and a reference lead is placed in the bath. These two probes are used to measure the voltage difference across the membrane of the cardiac cell. The characteristic time course of the transmembrane voltage measured experimentally is shown in Fig. S1. To extract APD from the voltage traces shown in Fig. S1, the difference between the timing of the upstroke of the voltage and 70% recovery back to the baseline voltage of the downstroke is determined. We refer to this as  $APD_{70}$ .  $APD_{70}$  is measured in units of time and is indicated by the solid line labeled  $APD$  in Fig. S1(a). Typically, the time between the recovery of the downstroke and the next subsequent upstroke is also measured. This is called the diastolic interval and is labeled in Fig. S1(a) with a D above the dotted line that indicates the width in units of time.

Comparing Figs. S1(a) and (b) (for  $\delta = 0$ ), the series of APDs are only slightly different in length reflecting the small difference in the basic cycle length (BCL). The morphology of the APD are identical. This is a crucial point because each  $B_0$  encompasses two distinct trends in  $\Gamma$  vs.  $\delta$  under alternate pacing. Specifically, for the action potentials shown in Fig. S1(a) with a steady state  $B_0 = 800 \text{ ms}$ ,  $\Gamma$  decreases as  $\delta$  decreases, as shown in Fig. S5(a). On the

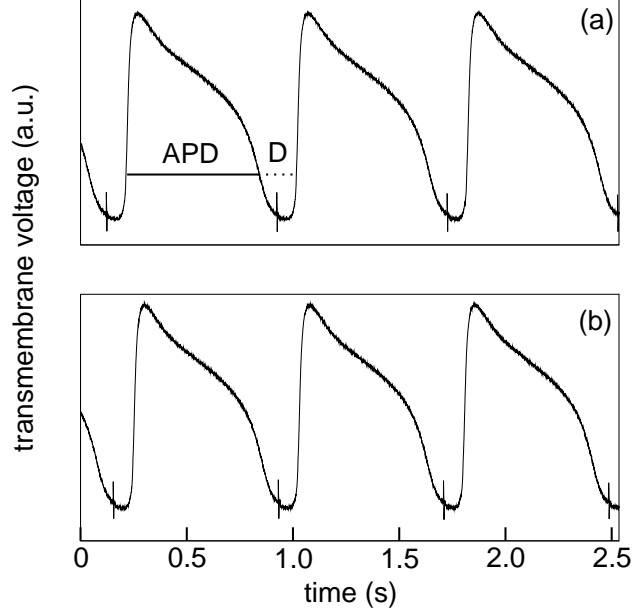


FIG. S1: A plot of action potentials (APs) for the data shown in Fig. 3(b) of Ref. [1] and Fig. S5. Steady state APs for  $B_0 = 800$  ms are shown in (a) and steady state APs for  $B_0 = 775$  ms are shown in (b).

other hand, for the action potentials shown in Fig. S1(b) with a steady state  $B_0 = 775$  ms,  $\Gamma$  increases as  $\delta$  decreases, as shown in Fig. S5(b). Nevertheless, the difference in the trends in  $\Gamma$  vs.  $\delta$  is not reflected in the action potential shape.

### $\Gamma$ vs. $\delta$ near the Bifurcation

Here we include a complete presentation of all the data from all trials that exhibit alternans. The data are classified into four categories: increasing trend ( $\Gamma$  increases and  $\delta$  decreases), shown in Fig. S2 and summarized in Table SI, decreasing trend ( $\Gamma$  decreases and  $\delta$  decreases), shown in Fig. S3 and summarized in Table SII, no-trend data (no significant variation in  $\Gamma$  as  $\delta$  varies) shown in Fig. S4 and summarized in Table SIII, and both increasing and decreasing data from one trial show in Fig. S5 (the same data presented in Fig. 3 of Ref. [1]) and summarized in Table SIV.

We use the Likelihood Ratio Test (LRT) [2, 3] to determine how to categorize the data. This procedure tests the null hypothesis ( $H_o$ ) that our data is randomly scattered about a mean. We chose to reject the null hypothesis if the computed p-value was less than 0.05. When the p-value is less than 0.05, the alternative hypothesis ( $H_a$ ) is accepted to be true. The alternative hypothesis is that we have four (in some cases three) unique data points

that are independent of each other. Verification of  $H_a$  indicates an increasing or decreasing trend in  $\Gamma$  vs.  $\delta$  and the distinction between the two trends is verified via a visual test.

The LRT is computed in the following way. The LRT statistic ( $\lambda$ ) is

$$\lambda = \frac{\max_{\mu} P(x_1, x_2, x_3, x_4 | H_o)}{\max_{\mu_1, \mu_2, \mu_3, \mu_4} P(x_1, x_2, x_3, x_4 | H_a)}, \quad (1)$$

where  $x_n$  ( $n = 1, 2, 3, 4$ ) correspond to the data (in some cases  $n = 1, 2, 3$  since we sometimes only have three data points). We maximize the numerator and denominator of Eq. 1 under the conditions of the null hypothesis ( $H_o$ ) and the alternative hypothesis ( $H_a$ ), respectively. The probability function is a Gaussian of the general form

$$P(x) = \frac{1}{\sigma\sqrt{2\pi}} e^{-(x-\mu)^2/2\sigma^2}, \quad (2)$$

where  $\sigma$  corresponds to the error in the data (in our case, this would vary between data points),  $x$  corresponds to the data and  $\mu$  is determined by the hypothesis. For the null hypothesis,  $\mu$  is the weighted mean computed as

$$\mu | H_o = \mu_o = \frac{\sum_{i=1}^n \frac{x_i}{\sigma_i^2}}{\sum_{i=1}^n \frac{1}{\sigma_i^2}}. \quad (3)$$

The numerator of Eq. 1 can then be computed by taking the product of Eq. 2 for each data point in the  $\Gamma$  vs.  $\delta$  plot, where  $\mu = \mu_o$ . This can be written as

$$\max_{\mu_o} P(x_1, x_2, x_3, x_4 | H_o) = \prod_{n=1}^4 \frac{1}{\sigma_n \sqrt{2\pi}} e^{-(x_n - \mu_o)^2 / 2\sigma_n^2}. \quad (4)$$

The product in Eq. 4 reduces to three terms in the case where we have three data points. To maximize the denominator in Eq. 1, let each value of  $\mu_n$  equal the corresponding data point  $x_n$ . Therefore, the denominator only depends on the uncertainty of each of the four data points (and in some cases three). The denominator can be rewritten as

$$\max_{\mu_1, \mu_2, \mu_3, \mu_4} P(x_1, x_2, x_3, x_4 | H_a) = \prod_{n=1}^4 \frac{1}{\sigma_n \sqrt{2\pi}}. \quad (5)$$

Taking the logarithm of Eq. 1 and in the limit where we have infinite number of data points allows for the following approximation

$$-2\ln(\lambda) \sim \chi_3^2, \quad (6)$$

where  $\chi_3^2$  is called a  $\chi$ -square distribution [4] with 3 degrees of freedom (the  $\chi$ -square distribution will have 2 degrees of freedom when we only have three data points). The  $\chi$ -square distribution can be expressed generically as

$$f(y|\nu) = \frac{y^{(\nu-2)/2} e^{-y/2}}{2^{\nu/2} \Gamma(\nu/2)}, \quad (7)$$

where  $y$  is a positive, independent variable,  $\nu$  corresponds to the number of degrees of freedom and  $\Gamma(\nu/2)$  is the gamma function. We compute the area under the  $\chi$ -squared distribution by integrating Eq. 7 from 0 to  $-2\ln\lambda$ , where  $-2\ln\lambda$  is computed for each trial. The p-value is then

$$\text{p-value} = 1 - \int_0^{-2\ln\lambda} \frac{t^{(\nu-2)/2} e^{-t/2}}{2^{\nu/2} \Gamma(\nu/2)} dt. \quad (8)$$

### *Categorization of Results*

This subsection is organized in the following way: a series of plots that fall into a specific category and a subsequent table to detail the findings within a particular category.

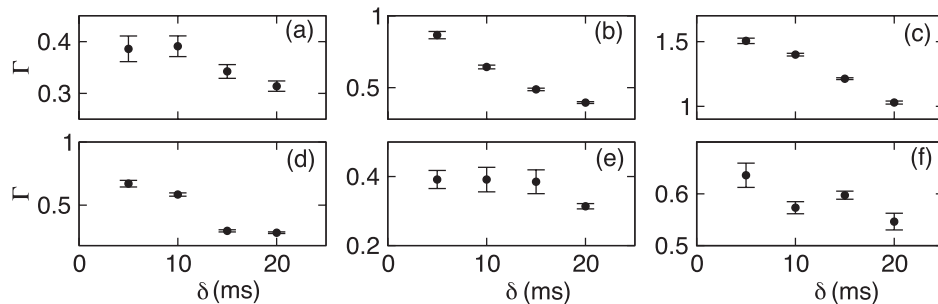


FIG. S2: Six trials from 4 separate frogs where the trend in  $\Gamma$  increases as  $\delta$  decreases. All figures are for the closest possible  $B_0$  to the bifurcation point to alternans.

Each table contains the following information (where the following bold lettering indicates the row label in the first column of the table): **frog #**, the **type** of trend (I:  $\Gamma$  increasing as

TABLE SI: This table outlines the properties from six trial in four frogs where an increasing trend is present. The order of columns 2-7 in this table correspond to Fig. S2(a)-(f) starting from the top and going left to right. This means that column 2 corresponds to Fig. S2(a) and column 7 corresponds to Fig. S2(f).

<b>frog #</b>	1	2	2	3	3	5
<b>type</b>	I	I	I	I	I	I
<b>p-value</b>	< 0.01	< 0.01	< 0.01	< 0.01	< 0.01	< 0.01
<b><math>B_o</math>(ms)</b>	750	750	300	600	680	300
<b><math>B_{bif}</math>(ms) range</b>	725-750	650-750	275-300	500-600	660-680	275-300
<b>step size (ms)</b>	25	50	25	100	20	25

TABLE SII: This table outlines the properties from three trial in two frogs where a decreasing trend is present. The second column specifies information for Fig. S3(a), the third column specifies information for Fig. S3(b) and the fourth column specifies information for fig. S3(c).

<b>frog #</b>	1	1	4
<b>type</b>	D	D	D
<b>p-value</b>	0.04	< 0.01	< 0.01
<b><math>B_o</math>(ms)</b>	750	700	500
<b><math>B_{bif}</math>(ms) range</b>	725-750	675-700	450-500
<b>step size (ms)</b>	25	25	50

$\delta$  decreases, D:  $\Gamma$  decreasing as  $\delta$  decreases, F: flat, or no trend in  $\Gamma$  vs  $\delta$ ), the **p-value** for a flat (or no-trend) null hypothesis as determined by a LRT, the  **$B_o$ (ms)** where the data was taken, a  **$B_{bif}$ (ms) range** that specifies the region that contains  $B_{bif}$  (bifurcation to alternans) since experimentally we cannot locate the exact point, and the **step size** taken for that particular trial.

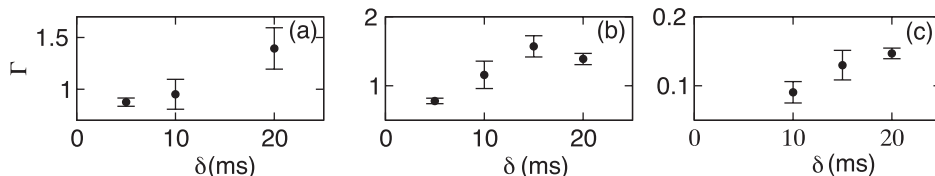


FIG. S3: Three trials from 2 separate frogs where the trend in  $\Gamma$  decreases as  $\delta$  delta decreases. All figures are for the closest possible  $B_0$  to the bifurcation point to alternans.

The increasing trend is the first featured. We have six examples of this displayed in three frogs (see fig. S2 and table SI). All p-values denoting an increasing trend are < 0.01. The

TABLE SIII: This table outlines the properties from two trial in two frogs where a flat trend is present. The second column specifies information for Fig. S4(a) and the third column specifies information for Fig. S4(b).

<b>frog #</b>	1	4
<b>type</b>	F	F
<b>p-value</b>	0.49	0.86
<b><math>B_o</math>(ms)</b>	500	575
<b><math>B_{bif}</math>(ms) range</b>	400-500	550-575
<b>step size (ms)</b>	100	25

decreasing trend is the second featured. We have three examples of this in two frogs (see fig. S3 and table SII). Notice that frog 1 appears in both the increasing and decreasing trends group. This indicates that, from frog 1, we were sometimes on the near side of the

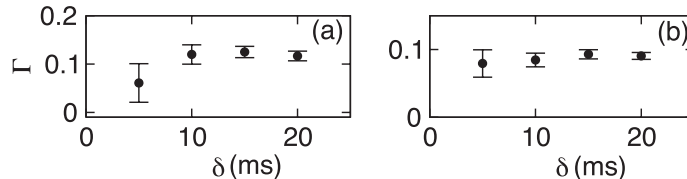


FIG. S4: Two trials from 2 separate frogs where the trend in  $\Gamma$  does not vary significantly as  $\delta$  is varied. All figures are for the closest possible  $B_0$  to the bifurcation point to alternans. These two plots raise the possibility that, under the unfolded border collision model, we are either very far from the bifurcation point or in region where the trend is beginning to switch from a decreasing trend to an increasing trend in  $\Gamma$  vs.  $\delta$ .

bifurcation point after the crossing in the unfolded border collision model (see Fig. 4 of Re. [1]) and other times we were beyond the crossing point so that the border-collision like trend was evident.

We also have two examples from two frogs that show no trend in  $\Gamma$  vs.  $\delta$  (see Fig. S4 and table SIII). This flat trend could be indicative of the crossing point where the trend flips between increasing and decreasing or it could indicate a significant distance from  $B_{bif}$  where the trend eventually flattens out as well. Finally, the data from Fig. 3 of Ref. [1] is also shown here (see Fig. S5 and table SIV). This includes the closest point to the bifurcation, where the trend in  $\Gamma$  vs.  $\delta$  is of the increasing type, and the next closest point where the trend is of the decreasing type. This data best illustrates the unfolded border collision

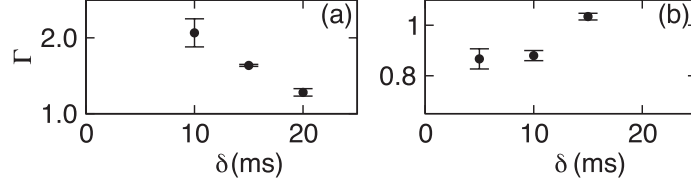


FIG. S5: Data from one trial in one frog that has been discussed in Ref. [1] in detail and is featured in Fig. 3 of Ref. [1]. The two figures are for the closest and second closest  $B_0$  to the bifurcation point to alternans. For  $B_0 = 775$  ms as show in (a), the trend in  $\Gamma$  is increasing as  $\delta$  decreases whereas the opposite holds for  $B_0 = 800$  ms as shown in (b). The entire data set (encompassing all values of  $B_0$ ) is plotted in Fig. 3 of the manuscript.

TABLE SIV: The table outlining the properties from one trial in one frog where both increasing and decreasing trends are present. The second column specifies information for fig. S5(a) and the third column specifies information for fig. S5(b).

<b>frog #</b>	1	1
<b>type</b>	I	D
<b>p-value</b>	< 0.01	< 0.01
<b><math>B_o</math>(ms)</b>	775	800
<b><math>B_{bif}</math>(ms) range</b>	750-775	750-775
<b>step size (ms)</b>	25	25

model. None the less, all the data presented here is consistent with an unfolded border collision type of bifurcation.

- 
- [1] C. Berger, X. Zhao, D. Schaeffer, H. Dobrovolny, W. Krassowska, and D. Gauthier. PRL, (2007).
- [2] G. Casella and R. L. Berger, *Statistical Inference* (Duxbury Advanced Series, Australia, 2002), Ch. 8.
- [3] Advice and analysis assisted by Statistician Michael Lavine, Duke University and Mathematician Mark Huber, Duke University. We greatly appreciate their insight and very valuable discussion.
- [4] R. Larsen and M. Marx, *An Introduction to Mathematical Statistics and its Applications* (Prentice-Hall, New Jersey, 1986), Ch. 7.